Key Engineering Materials
ISSN: 1662-9795, Vol. 658, pp 106-110
doi:10.4028/www.scientific.net/KEM.658.106

Submitted: 2014-12-11
Revised: 2015-03-10
Accepted: 2015-03-18
Online: 2015-07-29

Determination of Mechanical Adhesion Energy of Thermal Oxide Scales on Steel Produced from Medium and Thin Slabs using Tensile Test

Thanasak Nilsonthi

Department of Materials and Production Technology Engineering, Faculty of Engineering, King Mongkut's University of Technology North Bangkok, 1518 Pracharat 1 Road, Wongsawang, Bangsue, Bangkok 10800, Thailand

thanasakn@kmutnb.ac.th

Keywords: scale adhesion, tensile test, medium slab, thin slab

Abstract. The mechanical adhesion of thermal oxide scales formed on industrial hot-rolled steel strips produced through the electric-arc-furnace route was studied. The samples as-received steel were prepared with the specific shape fitting to the micro-tensile machine in the SEM chamber for observation of surface failure during the test. It was found that oxide transverse cracking and scale spallation are observed. This paper also presented a theoretical model for evaluate adhesion energy from strain and stress values at the first spallation. It was found that the oxide scales on the medium slab exhibited high mechanical adhesion energy. This might be due to the existence of oxide contained Si at steel-scale interfaces. It can promote adhesive interactions between steel-scale interfaces.

Introduction

Steel scraps as main raw materials are used to produce the steels by electric-arc-furnace (EAF) route. Slabs produced by this process might be classified by their thickness. The recycled slab can be either a medium slab in case that its thickness is ca. 80 to 100 mm, or a thin slab in case that its thickness is ca. 50 mm. In a hot rolling process, an oxide scale layer can be always formed on the steel strips surface. The scale structure consists of three layers as external layer of hematite (Fe_2O_3), an intermediate layer of magnetite (Fe_3O_4), and internal wustite (FeO) layer [1-4]. The surface quality of the final strip is required before further processing. The scales can be done by mechanical and/or chemical means. The scale adhesion behavior is several methods developed. The materials as thin shape can used the inverted blister test for measuring adhesion [5] and the three point bending test [6]. Our group has developed the macro-tensile and micro-tensile test [7-12]. The micro-tensile test was usually applied to assess the adhesion of scale on stainless steel. However, the oxide on stainless steel was mainly chromia [13-15] with the thickness used in our study less than 5 μm [16]. The present work adapted that method assess the adhesion of scale on low carbon steel which has a relatively thicker scale than those on stainless steel. No extensive work has been applied to measure scale adhesion of low carbon steels at room temperature, even though this property is of importance for surface quality of the hot-rolled steel product. The objective of the present paper was therefore to investigate the mechanical adhesion of scale on the hot-rolled steel strips produced from medium and thin slabs at room temperature by the micro-tensile test.

Experimental

The mechanical adhesion was evaluated for two hot-rolled low carbon steels. The steels were cut from strips obtained from slabs produced by the electric-arc-furnace route called in the present work medium and thin slabs. The thickness of the strips was 6 and 1.3 mm for the steel produced from medium and thin slabs respectively. Their chemical compositions are given in Table 1. The micro-

tensile test machine was used in this work for determining the strain at the first spallation and the evolution of the spalled fraction of scale. The samples were prepared by electro-erosion with the specific shape fitting to the machine sitting in the chamber of the scanning electron microscope (SEM). During tensile loading, the evaluation of the failure of the scale was monitored by SEM. The experimental set-up and quantification method of the adhesion energy of this test was described elsewhere [7,16].

Table 1 Chemical compositions of the studied materials (wt.%).

Slab	C	Si	Cu	Mn	Al	P	S	Fe
Medium	0.058	0.267	0.168	0.347	0.020	0.013	0.004	bal.
Thin	0.077	0.191	0.159	0.233	0.016	0.006	0.004	bal.

Results and Discussion

For the mechanical adhesion energy of medium and thin slabs, Fig. 1 depicts the surface of scales on the steel produced from the medium and thin slabs subjected to the imposed strain. SEM image in each column shows the comparative scale surface of the steel after straining by the different values. During tensile loading, transverse cracks perpendicular to the tensile loading were first observed, followed by local scale spallation. It was also seen that initial cracks existed in scale on the steel produced from the medium slab, while no considerable cracks were observed on scale of the steel produced from the thin slab.

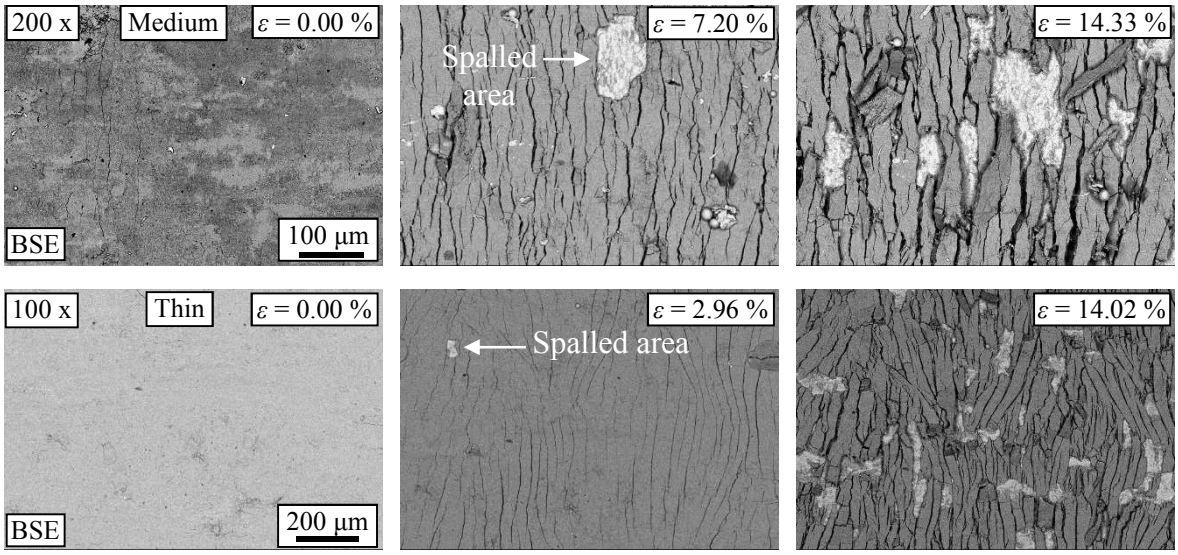

Fig. 1 Evolution of scale failure on medium slab (upper) and thin slab (lower).

The critical strains at the first spallation of the steel produced from the medium slab was 5.80 ± 1.41%. This value was higher than that of the steel produced from the thin slab which was 3.67 ± 0.71%. The averaged thicknesses of scales on steels produced from medium and thin slabs were 12 and 9 μm respectively.

To asses scale adhesion, mechanical adhesion energy at the first spallation can be given by [17]

$$G_i = W_{total} \cdot e \tag{1}$$

where G_i is the mechanical adhesion energy (J.m^{-2}), W_{total} is the total elastic stored energy attaining the energy requires to form a new surface at the metal-scale interface (J.m^{-3}), e is the oxide scale thickness (m). The total stored energy can be derived by stress-strain curve of the oxide as follows. The stress-strain evolution during the test is typically existed in both x and y directions parallel to the interface (x = tensile axis, y = transverse tensile axis), while that in z axis (perpendicular interface) is assumed to be zero. The mechanical behaviour of the metal was initially elastically deformed and then subjected to a plastic deformation, while the oxide was still elastic until the first spallation takes place. The present study refers to metal by the subscript s (substrate) and to oxide by the subscript f (film). The second subscript indicates the main axis (x and y). The superscript indicates *res* for residual stress, *el* and *pl* for elastic and plastic behaviours of the metal.

The stored energy of film in both x and y directions can be calculated by the simple relation (2) [16]. Stored energy development in film is considered in the three successive stages as shown in Table 2.

$$W_{total} = \int \sigma \cdot d\varepsilon = \sum W_{fx} + \sum W_{fy} \tag{2}$$

Table 2 The stored energy of film in both x and y directions of each stage [16].

Stage 1, the accumulation of residual stress due to the film grows and cools down. $W_{fx}^{res} = W_{fy}^{res} = \frac{1}{2}\sigma^{res}\varepsilon^{res} = \frac{\left(\sigma^{res}\right)^2}{2M_f}$ with $M_f = \frac{E_f}{1-\nu_f}$
Stage 2, substrate and film are in tension elastically. $W_{fx}^{el} = \frac{1}{2}\sigma_{fx}^{el}\varepsilon_{fx}^{el} = \frac{M_f^{'}}{2}\left(1-\nu_f\cdot\nu_s\right)\left(\varepsilon_{fx}^{el}\right)^2$ $W_{fy}^{el} = \frac{1}{2}\sigma_{fy}^{el}\varepsilon_{fy}^{el} = \frac{M_f^{'}}{2}\left\|\nu_f-\nu_s\right\|\left(\varepsilon_{fx}^{el}\right)^2$ with $M_f^{'} = \frac{E_f}{1-\nu_f^2}$
Stage 3, substrate and film are in tension. Substrate is deformed plastically but film is still elastic until the first spalled. $W_{fx}^{pl} = \frac{1}{2}M_f^{'}\left(\varepsilon_{fx}^{pl}\right)^2 + 2M_f^{'}\nu_f\left(\sqrt{1+\varepsilon_{fx}^{pl}}-1\right) - M_f^{'}\nu_f\varepsilon_{fx}^{pl}$ $W_{fy}^{pl} = \frac{M_f^{'}\left(\varepsilon_{fy}^{pl}\right)^2}{2\left(1+\varepsilon_{fy}^{pl}\right)}\left(1+\varepsilon_{fy}^{pl}-2\nu_f\right)$ whereas $\varepsilon_{fy}^{pl} = \sqrt{\frac{1}{1+\varepsilon_{fx}^{pl}}}-1$

During tensile loading, substrate is in tension elastically until to limit of elasticity ($\varepsilon_s^{el,\lim}$), and then is plastic deformation, whereas film is still elastically deformed until the first spallation takes place. Therefore, strain of film in parallel to x axis of the plastic of stored energy (ε_{fx}^{pl}) can be written as $\varepsilon_{fx}^{pl} = \varepsilon_{fs} - \varepsilon_{fx}^{el}$. where ε_{fs} is strain at the first spallation. The mechanical parameters for quantifying the stored energy are as the following. The Young's modulus of the iron oxide (E_f) is

210 GPa, the Poisson's ratio of metal and oxide are 0.3 ($\nu_s = \nu_f = 0.3$) by assuming perfectly adherent metal/oxide, the Young's modulus of the metal (E_s) is 210 GPa, the compressive residual stress of oxide (σ^{res}) is – 0.2 GPa, the strain at limit of elasticity of iron oxide (ε_{fx}^{el}) is 0.00095 (0.095%).

The mechanical adhesion energy and the strain initiating the first spallation of the studied samples are shown in Fig. 2. The mechanical adhesion energies for scale on the steel produced from the medium slab was 1535 ± 711 J.m^{-2}. These are higher than that for scale on the steel produced from the thin slab which was 448 ± 169 J.m^{-2}. These results indicate higher mechanical adhesion of scale actually formed on the medium slab than that of scale actually formed on the thin slab.

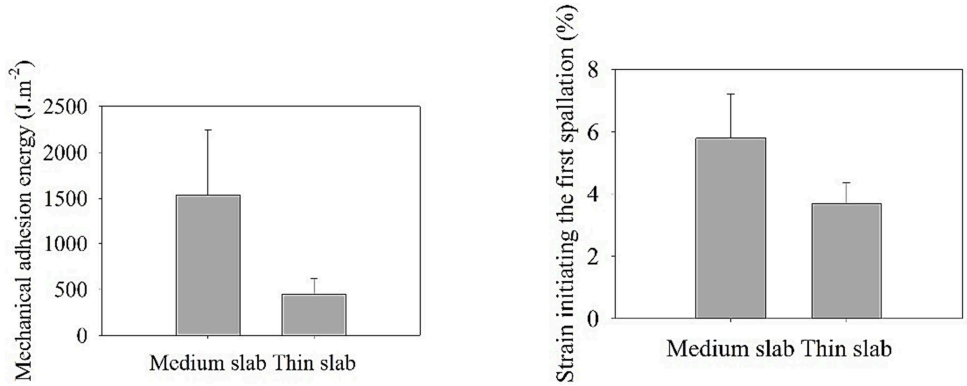

Fig. 2 Mechanical adhesion energy (left) and strain initiating the first spallation (right) of scale on the medium and thin slabs.

For discussion on the role of silicon on formation and adhesion of scale on steel substrate, Fig. 3 depicts the scale on the steel produced from the medium slab after the tensile test. The EDS spectrum on steel substrate includes the peaks of Fe, O as well as Si. This indicated the existence of oxide containing Si at the steel-scale interface. The fayalite (Fe_2SiO_4) was found at the steel-scale interface could promotes scale adhesion that reported by [2,18,19].

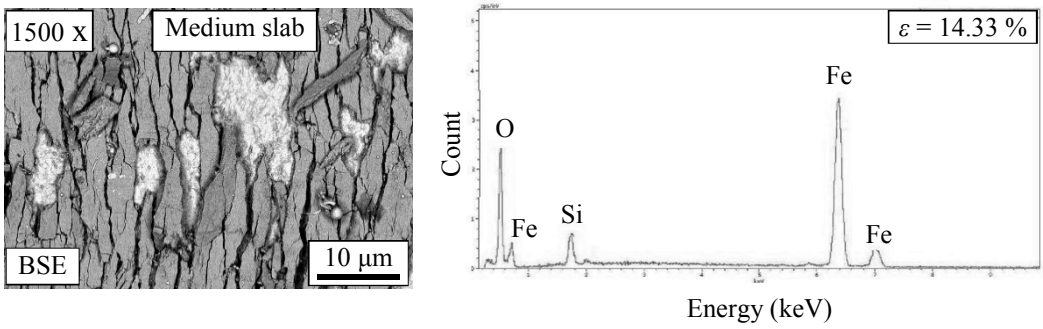

Fig. 3 Surface of medium slab after tensile test (left) and EDS pattern (right).

Summary

The micro-tensile machine operating in a SEM chamber was applied to observe oxide scale failure. The transverse cracks were first observed, followed by scale spallation. The mechanical adhesion energies of scale on the steels produced by medium and thin slabs were 1535 and 448 J.m^{-2} respectively. These results indicated the higher mechanical adhesion of scale on the medium slab.

Acknowledgements

The author acknowledge Faculty of Engineering, King Mongkut's University of Technology North Bangkok grant Contract no. 57-10-09-217. Professors A. Galerie and Y. Wouters is acknowledged for the kind supervision of research at University of Grenoble, France.

References

[1] R.Y Chan, W.Y.D. Yuen, ISIJ Inter. 45 (2005) 52-59.

[2] Y.-L Yang, C.-H. Yang, S.-N. Lin, C.-H. Chen, W.-T. Tsai, Mater. Che. Phy. 112 (2008) 566-571.

[3] A. Segawa, Mater Sci Forum. 696 (2011) 150-155.

[4] S. Chandra-ambhorn, T. Nilsonthi, Y. Wouters, A. Galerie, Corros. Sci. 87 (2014) 101-110.

[5] J. Mougin, M. Dupeux, L. Antoni, A. Galerie, Mater. Sci. Eng. A. 359 (2003) 44-51.

[6] A. Galerie, F. Toscan, E. N'Dah, K. Przybylski, Y. Wouters, M. Dupeux, Mater. Sci. Forum. 461-464 (2004) 631-638.

[7] F. Toscan, L. Antoni, Y. Wouters, M. Dupeux, A. Galerie, Mater. Sci. Forum. 461-464 (2004) 705-712.

[8] S. Chandra-ambhorn, T. Nilsonthi, Y. Madi, A. Galerie, Key Eng. Mater. 410-411 (2009) 187-193.

[9] S. Chandra-ambhorn, T. Somphakdee, W. Chandra-ambhorn, Mater. Sci. Forum. 696 (2011) 156-161.

[10] K. Ngamkham, S. Niltawach, S. Chandra-ambhorn, Key Eng. Mater. 462-463 (2011) 407-412.

[11] S. Chandra-ambhorn, K. Ngamkham, N. Jiratthanakul, Oxid. Met. 80 (2013) 61-72.

[12] T. Nilsonthi, S. Chandra-ambhorn, Y. Wouters, A. Galerie, Oxid. Met. 79 (2013) 325-335.

[13] P. Promdirek, G. Lothongkum, S. Chandra-ambhorn, Y. Wouters, A. Galerie, Mater. Corros. 62 (2011) 616-622.

[14] W. Wongpromrat, H. Thaikan, W. Chandra-ambhorn, S. Chandra-ambhorn, Oxid. Met. 79 (2013) 529-540.

[15] P. Promdirek, G. Lothongkum, S. Chandra-ambhorn, Y. Wouters, A. Galerie, Oxid. Met. 81 (2014) 315-329.

[16] S. Chandra-ambhorn, F. Roussel-Dherbey, F. Toscan, Y. Wouters, A. Galerie, M. Dupeux, Mater. Sci. Tech. 23 (2007) 497-501.

[17] H.E. Evans, Inter. Mater. Rev. 40 (1995) 1-40.

[18] S. Taniguchi, K. Yamamoto, D. Megumi, T. Shibata, Mater. Sci. Eng. A. 308 (2001) 250-257.

[19] T. Nilsonthi, J. Tungtrongpairoj, S. Chandra-ambhorn, Y. Wouters, A. Galerie, Steel Res. Inter. (2012) 987-990.

Metallurgy and Materials Engineering
10.4028/www.scientific.net/KEM.658

Determination of Mechanical Adhesion Energy of Thermal Oxide Scales on Steel Produced from Medium and Thin Slabs Using Tensile Test
10.4028/www.scientific.net/KEM.658.106

DOI References
[1] R. Y Chan, W.Y.D. Yuen, ISIJ Inter. 45 (2005) 52-59.
10.2355/isijinternational.45.52
[3] A. Segawa, Mater Sci Forum. 696 (2011) 150-155.
10.4028/www.scientific.net/MSF.696.150
[4] S. Chandra-ambhorn, T. Nilsonthi, Y. Wouters, A. Galerie, Corros. Sci. 87 (2014) 101-110.
10.1016/j.corsci.2014.06.018
[5] J. Mougin, M. Dupeux, L. Antoni, A. Galerie, Mater. Sci. Eng. A. 359 (2003) 44-51.
10.1016/S0921-5093(03)00355-1
[6] A. Galerie, F. Toscan, E. N'Dah, K. Przybylski, Y. Wouters, M. Dupeux, Mater. Sci. Forum. 461-464 (2004) 631-638.
10.4028/www.scientific.net/MSF.461-464.631
[7] F. Toscan, L. Antoni, Y. Wouters, M. Dupeux, A. Galerie, Mater. Sci. Forum. 461-464 (2004) 705-712.
10.4028/www.scientific.net/MSF.461-464.705
[9] S. Chandra-ambhorn, T. Somphakdee, W. Chandra-ambhorn, Mater. Sci. Forum. 696 (2011) 156-161.
10.4028/www.scientific.net/MSF.696.156
[10] K. Ngamkham, S. Niltawach, S. Chandra-ambhorn, Key Eng. Mater. 462-463 (2011) 407-412.
10.4028/www.scientific.net/KEM.462-463.407
[11] S. Chandra-ambhorn, K. Ngamkham, N. Jiratthanakul, Oxid. Met. 80 (2013) 61-72.
10.1007/s11085-013-9370-6
[12] T. Nilsonthi, S. Chandra-ambhorn, Y. Wouters, A. Galerie, Oxid. Met. 79 (2013) 325-335.
10.1007/s11085-012-9356-9
[13] P. Promdirek, G. Lothongkum, S. Chandra-ambhorn, Y. Wouters, A. Galerie, Mater. Corros. 62 (2011) 616-622.
10.1002/maco.201005878
[14] W. Wongpromrat, H. Thaikan, W. Chandra-ambhorn, S. Chandra-ambhorn, Oxid. Met. 79 (2013) 529-540.
10.1007/s11085-013-9379-x
[15] P. Promdirek, G. Lothongkum, S. Chandra-ambhorn, Y. Wouters, A. Galerie, Oxid. Met. 81 (2014) 315-329.
10.1007/s11085-013-9432-9
[16] S. Chandra-ambhorn, F. Roussel-Dherbey, F. Toscan, Y. Wouters, A. Galerie, M. Dupeux, Mater. Sci. Tech. 23 (2007) 497-501.
10.1179/174328407X168964
[17] H.E. Evans, Inter. Mater. Rev. 40 (1995) 1-40.
10.1179/imr.1995.40.1.1
[18] S. Taniguchi, K. Yamamoto, D. Megumi, T. Shibata, Mater. Sci. Eng. A. 308 (2001) 250-257.
10.1016/S0921-5093(00)01977-8